Dysregulation of the ALS-associated gene TDP-43 leads to neuronal death and degeneration in mice

Lionel M. Igaz, Linda K. Kwong, Edward B. Lee, Alice Chen-Plotkin, Eric Swanson, Travis Unger, Joe Malunda, Yan Xu, Matthew J. Winton, John Q. Trojanowski, and Virginia M.-Y. Lee

Center for Neurodegenerative Disease Research, Department of Pathology and Laboratory Medicine, and Institute on Aging, University of Pennsylvania School of Medicine, Philadelphia, Pennsylvania, USA.

Amyotrophic lateral sclerosis (ALS) and frontotemporal lobar degeneration (FTLD) are characterized by cytoplasmic protein aggregates in the brain and spinal cord that include TAR-DNA binding protein 43 (TDP-43). TDP-43 is normally localized in the nucleus with roles in the regulation of gene expression, and pathological cytoplasmic aggregates are associated with depletion of nuclear protein. Here, we generated transgenic mice expressing human TDP-43 with a defective nuclear localization signal in the forebrain (hTDP-43-ΔNLS), and compared them with mice expressing WT hTDP-43 (hTDP-43-WT) to determine the effects of mislocalized cytoplasmic TDP-43 on neuronal viability. Expression of either hTDP-43-ΔNLS or hTDP-43-WT led to neuron loss in selectively vulnerable forebrain regions, corticospinal tract degeneration, and motor spasticity recapitulating key aspects of FTLD and primary lateral sclerosis. Only rare cytoplasmic phosphorylated and ubiquitinated TDP-43 inclusions were seen in hTDP-43-ΔNLS mice, suggesting that cytoplasmic inclusions were not required to induce neuronal death. Instead, neurodegeneration in hTDP-43 and hTDP-43-ΔNLS–expressing neurons was accompanied by a dramatic downregulation of the endogenous mouse TDP-43. Moreover, mice expressing hTDP-43-ΔNLS exhibited profound changes in gene expression in cortical neurons. Our data suggest that perturbation of endogenous nuclear TDP-43 results in loss of normal TDP-43 function(s) and gene regulatory pathways, culminating in degeneration of selectively vulnerable affected neurons.

Introduction

Frontotemporal lobar degeneration (FTLD) and amyotrophic lateral sclerosis (ALS) are characterized by the presence of ubiquitin-positive inclusions (1). These inclusions are found in the brain and spinal cord of ALS patients as well as in patients with a major subtype of FTLD designated FTLD-TDP because these inclusions were shown to be comprised of the TAR-DNA binding protein 43 (TDP-43) (2). Since (a) cognitive abnormalities or dementia consistent with FTLD are increasingly recognized in ALS patients, (b) some FTLD patients develop MND, and (c) cytoplasmic TDP-43 aggregates are found in the brain and spinal cord of both ALS and FTLD-TDP patients, TDP-43 pathology appears to define a single neurodegenerative disorder (TDP-43 proteinopathy) with a spectrum of clinical manifestations (3–5). The importance of TDP-43 in the pathogenesis of these diseases is supported by the presence of autosomal dominant mutations in the *TARDBP* gene associated with ALS and FTLD (6).

Human TDP-43 (hTDP-43) is a highly conserved and ubiquitously expressed 414–amino acid nuclear protein that binds to both DNA and RNA (7, 8). TDP-43 is implicated in repression of gene transcription, regulation of exon splicing, and nuclear body functions (for a summary see recent reviews, refs. 4 and 6). Pathological TDP-43 can be abnormally cleaved, phosphorylated, and ubiquitinated, and most TDP-43 aggregates are mislocalized outside the nucleus within the cytoplasm or neurites (2). Interestingly, cells that develop TDP-43 accumulations show a dramatic depletion of normal nuclear TDP-43. Thus, both gain and loss of functions are potential disease mechanisms, either due to the loss of normal nuclear TDP-43 expression, cytoplasmic mislocalization, or cytoplasmic aggregation (2, 9, 10).

To mimic this nuclear clearance and to model the formation of TDP-43 cytoplasmic aggregates, we have shown that expression of hTDP-43 with mutated nuclear localization signals (hTDP-43-ΔNLS) in cultured cells reduces endogenous nuclear TDP-43 and accumulates as cytoplasmic aggregates (11). In vivo mouse models with TDP-43 knockout or overexpression have also been reported. *Tardbp*-null mice are embryonic lethal (12–15), and conditional *Tardbp* null mice exhibit rapid postnatal death associated with aberrations in fat metabolism (15). Tg mice with overexpression of human or mouse TDP-43-WT as well as mice expressing TDP-43 harboring disease-associated mutations have been reported to show TDP-43 pathologies associated with motor neuron degeneration reminiscent of ALS or FTLD-TDP (16–20). However, the effects of cytoplasmic TDP-43 expression on the formation of cytoplasmic aggregates, neurotoxicity, and normal nuclear TDP-43 protein on initiating neurodegeneration have not been addressed in vivo.

Here, we generated Tg mice with inducible forebrain overexpression of hTDP-43-ΔNLS using the Camk2a tetracycline transactivator (Camk2a tetO) to specifically model cytoplasmic mislocalization of TDP-43 and interrogate the consequences of this abnormal distribution of TDP-43 in the presence or absence of TDP-43 aggregates. We found profound neuron loss in specific regions, in particular, cortex (including motor cortex) and hippocampus, with corticospinal tract (CST) degeneration and a spastic motoric phenotype, all of which recapitulate key aspects of FTLD
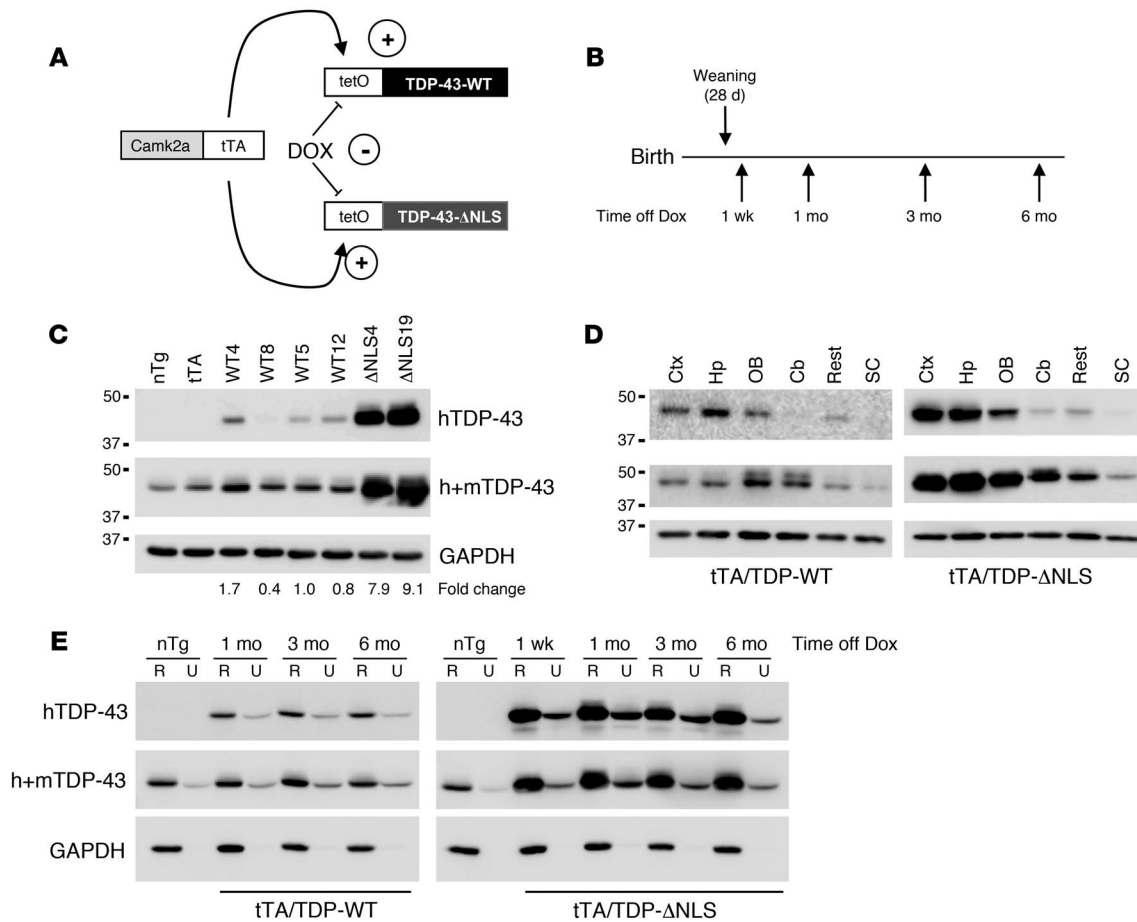
Figure 1
Generation and biochemical characterization of inducible TDP-43 Tg mice. (**A**) Generation of conditional Tg mice. Camk2a-tTA mice were crossed with tetO-TDP-WT or tetO-TDP-ΔNLS mice. In bigenic mice, Dox inhibits tTA binding to the tetracycline-responsive promoter element (tetO), repressing hTDP-43 expression. (**B**) Dox was removed at weaning (P28) followed by analysis at the indicated time points. (**C**) Expression of hTDP-43 in Tg mice. Immunoblot of hTDP-43 or total TDP-43 (h+mTDP-43) in cortical RIPA extracts (1 month off Dox) of nTg, tTA, tTA/TDP-WT (WT4, WT8, WT5 and WT12), and tTA/TDP-ΔNLS mice (ΔNLS4 and ΔNLS19) showed variable expression of hTDP-43. GAPDH is a loading control. Fold expression relative to nTg and tTA control mice is shown, as described in Methods. (**D**) Regional expression of hTDP-43. RIPA extracts from different brain regions of tTA/TDP-WT or tTA/TDP-ΔNLS mice (1 month off Dox) were immunoblotted for hTDP-43, h+m TDP-43, and GAPDH. Ctx, cerebral cortex; Hp, hippocampus; OB, olfactory bulb; Cb, cerebellum; Rest, brain stem plus subcortical gray regions; SC, spinal cord. (**E**) Low levels of insoluble hTDP-43. Sequential cortical extracts from tTA/TDP-WT and tTA/TDP-ΔNLS mice of increasing time off Dox were immunoblotted for hTDP-43 showing low levels of TDP-43 in urea fractions. Urea lysates were loaded at 4× relative to RIPA lysates so that the low level of insoluble TDP-43 could be seen. R, RIPA; U, urea. *n* = at least 3 animals per group analyzed in **C**–**E**.

and primary lateral sclerosis (PLS). However, only small numbers of phosphorylated and ubiquitinated cytoplasmic hTDP-43 aggregates are found in hTDP-43-ΔNLS Tg mice, and they do not correlate with the observed profound neurotoxicity. Instead, a dramatic loss of endogenous nuclear mouse TDP-43 (mTDP-43) was the only correlate to neurodegeneration in hTDP-43-ΔNLS–expressing mice. Significantly, this was associated with a strikingly abnormal and selective upregulation of chromatin assembly genes in hTDP-43-ΔNLS Tg mice. We conclude that endogenous nuclear TDP-43 is highly regulated and that perturbation of nuclear TDP-43 is associated with profound alterations in gene expression and cell death.

Results

Generation of Tg mice overexpressing hTDP-43-WT and hTDP-43-ΔNLS proteins. To create conditional mouse models of TDP-43 proteinop-

athies, we generated Tg mice expressing hTDP-43-ΔNLS and its control counterpart hTDP-43-WT using CaMK2α promoter elements to drive tet-off tTA (Camk2a-tTA) and a tetracycline responsive promoter to drive hTDP-43 expression (tetO-hTDP-43; Figure 1A) (21–23). Bigenic mice (Camk2a-tTA x tetO-hTDP-43) were maintained on Doxycycline (Dox) to inhibit transgene expression until 28 days of age when they were switched to a Dox-free diet and sacrificed at the designated time points off Dox (Figure 1B).

We identified 2 lines overexpressing hTDP-43-ΔNLS (bigenic mice designated tTA/TDP-ΔNLS) and 4 lines overexpressing hTDP-43-WT (bigenic mice designated tTA/TDP-WT) that expressed differing levels of TDP-43, ranging from 8- to 9-fold over endogenous mTDP-43 for tTA/TDP-ΔNLS mice and from 0.4- to 1.7-fold over endogenous mTDP-43 for tTA/TDP-WT mice (Figure 1C). We selected 1 line of tTA/TDP-ΔNLS (ΔNLS4) for
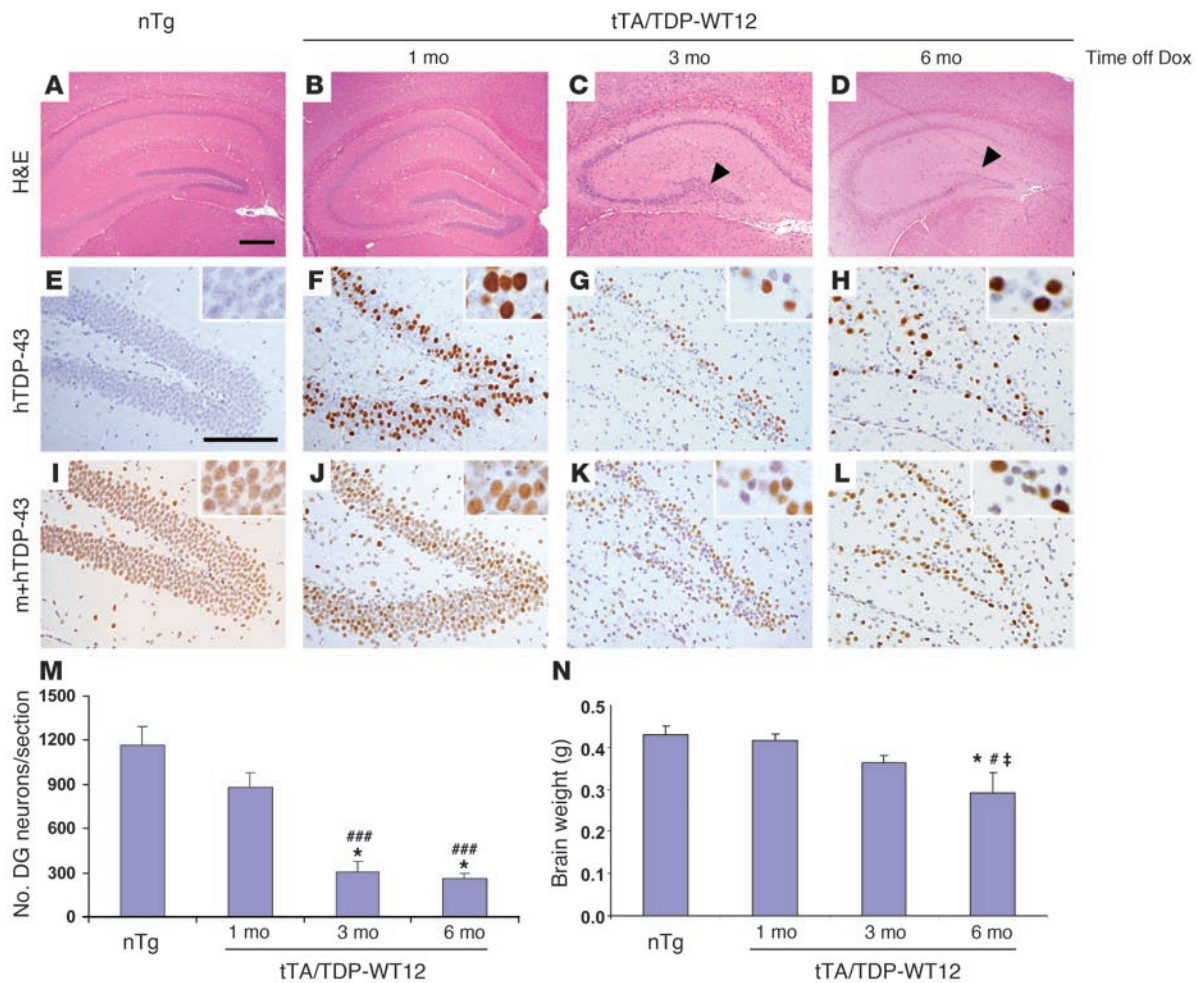
Figure 2
Neuron loss and cerebral atrophy in tTA/TDP-WT mice. (**A–L**) Expression of hTDP-43 and time-dependent cell loss in tTA/TDP-WT12 mice. (**A–D**) H&E sections of nTg (**A**) and tTA/TDP-WT12 (**B–D**) brain revealed time-dependent hippocampal neuron loss in bigenic mice. Note the loss of DG neurons as indicated by arrowheads. (**E–L**) Nuclear expression of hTDP-43. IHC for hTDP-43 (**E–H**) and h+mTDP-43 (**I–L**) showed mosaic nuclear expression of hTDP-43 in tTA/TDP-WT12 and a severe thinning of the DG cell layer after 3 to 6 months off Dox. Insets in **E–L** display higher magnification of DG neurons. Scale bars: 500 μm (**A–D**); 200 μm (**E–L**). (**M**) Loss of DG neurons in tTA/TDP-WT12 mice. Quantification of DG neurons shows progressive neuron loss in tTA/TDP-WT12 mice. (**N**) Time-dependent brain atrophy in tTA/TDP-WT12 mice. There was a progressive reduction in total brain weight in tTA/TDP-WT12 mice. Data in **M** and **N** represent mean ± SEM ($n = 3–4$ per group). *Significantly different from nTg ($P < 0.001$); ###significantly different from 1 month off Dox ($P < 0.001$); #significantly different from 1 month off Dox ($P < 0.05$); ‡significantly different from 3 months off Dox ($P < 0.05$).

in-depth analysis with the tTA/TDP-WT12 line as a control line, although the other Tg lines also were studied to ensure consistency of the relationship between phenotype and expression levels. Single Tg mice (tetO-TDP-ΔNLS or tetO-TDP-WT) showed little to no hTDP-43 expression indicative of very low tetO activity or "leakiness" (data not shown).

Mice showed neuronal expression predominantly, albeit not exclusively, in forebrain structures, consistent with the properties of the Camk2a promoter (21, 22). To demonstrate the regional differences in TDP-43 expression, protein lysates were analyzed using antibodies specific for hTDP-43 and antibodies recognizing both hTDP-43 and endogenous mTDP-43 (h+mTDP-43). High TDP-43 expression was found in cortex, hippocampus, and olfactory bulb, while cerebellum, subcortical regions/brain stem, and spinal cord displayed no or barely detectable hTDP-43 (Figure 1D). Sequen-

tial extraction using RIPA and urea buffers of cortex from bigenic WT12 and ΔNLS4 Tg mice showed the majority of hTDP-43 and mTDP-43 protein was recovered in the RIPA fraction (Figure 1E). However, low levels of TDP-43 (<10%) were detected in the urea fraction (Figure 1E), and C-terminal TDP-43 fragments (CTFs) were not found in any line at any of the time points examined (Supplemental Figure 1; supplemental material available online with this article; doi:10.1172/JCI44867DS1). Importantly, all tTA/TDP-WT and tTA/TDP-ΔNLS lines showed nearly complete suppression of transgene under constant Dox treatment (data not shown).

tTA/TDP-WT mice show progressive neurodegeneration. Overexpression of TDP-43-WT protein is known to be neurotoxic (16–20). To determine whether hTDP-43-WT exhibited similar neurotoxicity in our conditional WT12 line, a time course of neuron loss and the distribution of hTDP-43-WT protein was assessed by histological
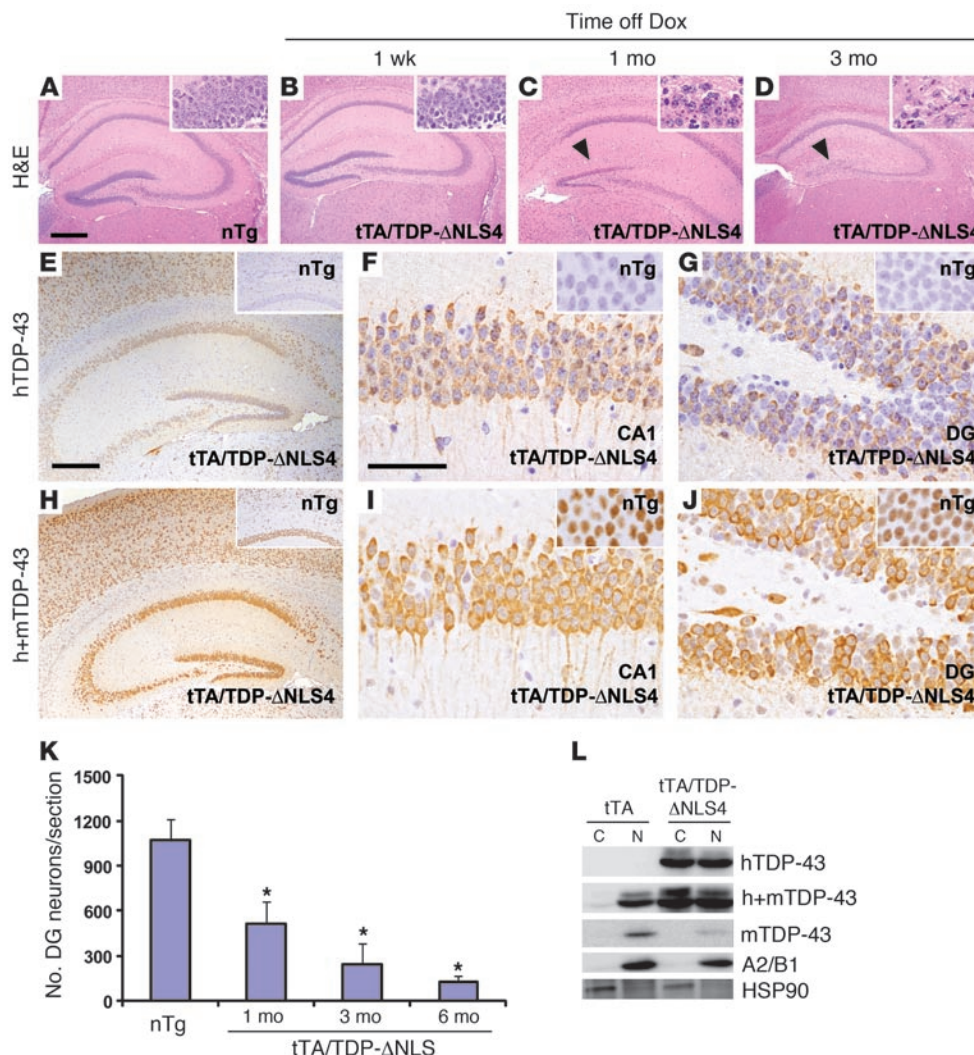
Figure 3

Cytoplasmic hTDP-43 expression and progressive neuronal loss in tTA/TDP-ΔNLS mice. (**A**–**D**) Progressive neuron loss in tTA/TDP-ΔNLS4 mice. Hippocampal H&E sections of nTg (**A**) and tTA/TDP-ΔNLS (**B**) mice show a progressive DG neuron loss evident from 1 month off Dox (arrowhead highlights DG degeneration). (**E**–**J**) Cytoplasmic TDP-43 expression in tTA/TDP-ΔNLS hippocampus. IHC for hTDP-43 (**E**–**G**) or h+m TDP-43 (**H**–**J**) was performed on hippocampal sections from bigenic mice 1 week off Dox showing predominantly cytoplasmic expression of TDP-43. Insets show nTg mice with no hTDP-43 expression and nuclear h+mTDP-43 expression. Scale bars: 500 μm; (**A**–**D**, **E** and **H**); 200 μm (**F**, **G**, **I**, and **J**). (**K**) Loss of DG neurons in tTA/TDP-ΔNLS4 mice. Quantification of DG neurons shows progressive neuronal loss in tTA/TDP-ΔNLS mice. Data shown represent mean ± SEM (*n* = 3–4 per group). *Significantly different from nTg (*P* < 0.001). (**L**) Immunoblot analysis of enriched cytoplasmic (C) and nuclear (N) fractions isolated from cortical extracts of monogenic tTA and 2-month-old bigenic tTA/TDP-ΔNLS mice 10 days off Dox showing the presence of hTDP-43 in both fractions in tTA/TDP-ΔNLS. Note endogenous mTDP-43 is predominately nuclear. Nuclear hnRNP A2/B1 and cytoplasmic HSP90 indicated that the fractions are well separated.

and immunohistochemical (IHC) analyses of these mice (Figure 2). Although nTg and single Tg littermates never showed signs of neurodegeneration, H&E-stained sections of tTA/TDP-WT brain showed time-dependent neuron loss in the hippocampal dentate gyrus (DG) and neocortex beginning at about 1 month, and this became progressively more severe from 3 to 6 months (Figure 2, A and D). Quantification of DG neuron loss showed approximately 20% loss of DG neurons at 1 month and approximately 75% loss by 3 months after Dox removal, which was paralleled by progressive brain atrophy as assessed by histology and total brain weight (Figure 2, M and N). Astrocytic and microglial activation were seen in

cortex and hippocampus by IHC with antibodies to glial fibrillary acidic protein (GFAP) and Iba-1 as early as 1 month off Dox (Supplemental Figure 2A and data not shown). Importantly, WT8 mice (low expressors) showed no detectable neuron loss at 3–4 months in contrast with WT4 mice (high expressors), which showed DG neurodegeneration as early as 7–10 days after Dox removal (data not shown). This suggests that there may be a threshold effect, with neurodegeneration occurring as a function of higher levels of exogenous hTDP-43 expression.

IHC for hTDP-43-WT in line WT12 revealed predominantly nuclear localization (Figure 2, F–H), with a mosaic pattern rang-
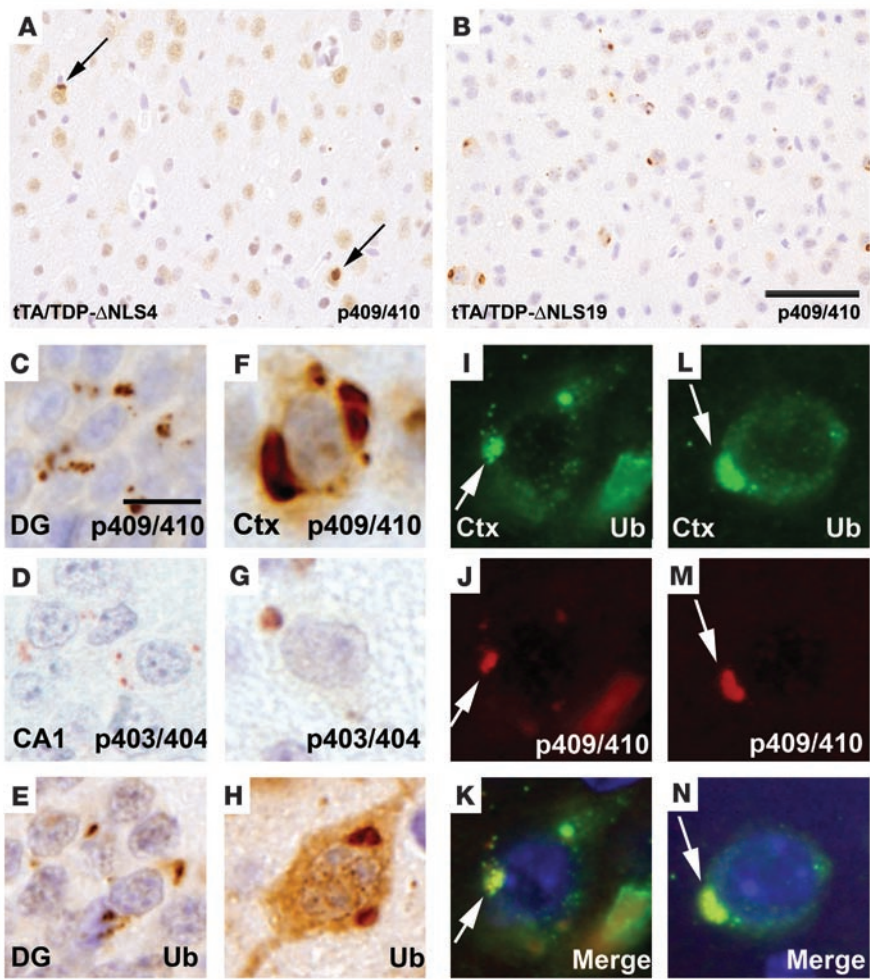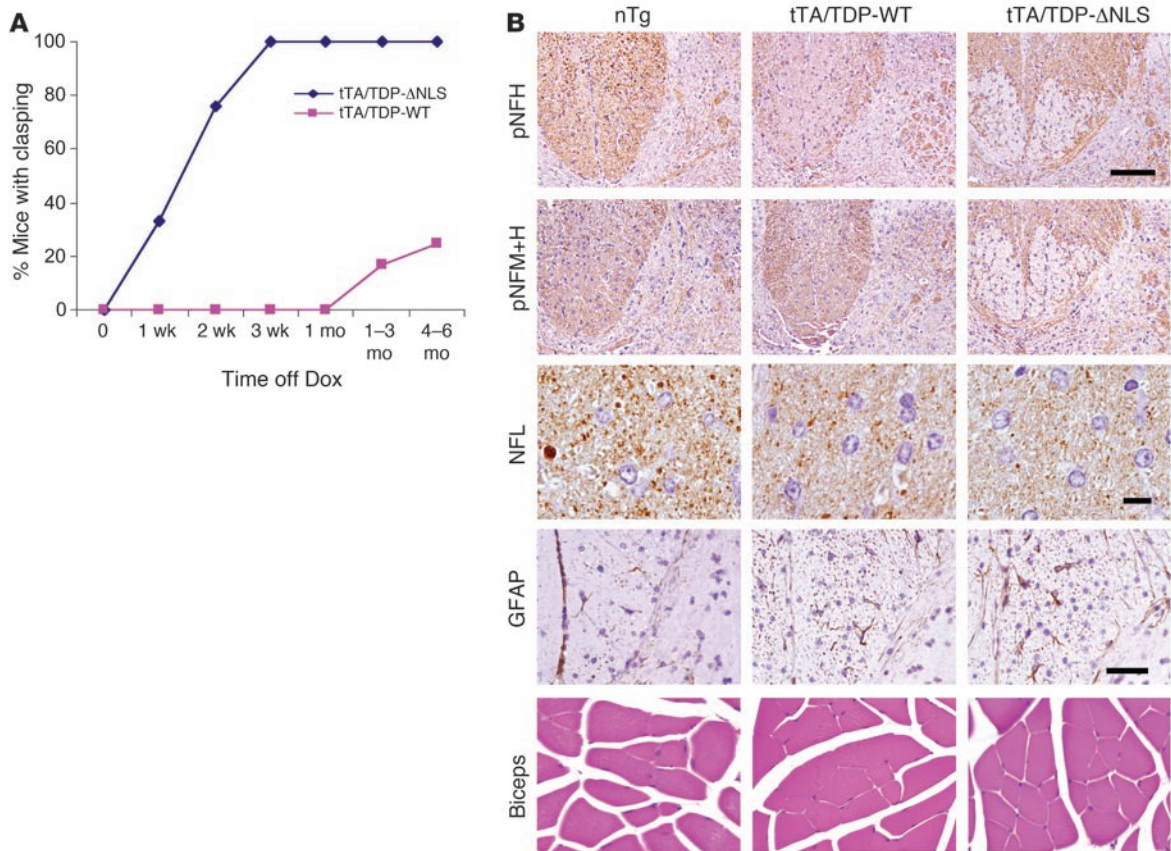
Figure 4
TDP-43 aggregates are phosphorylated and ubiquitinated in tTA/TDP-ΔNLS mice. (**A**–**H**) TDP-43 aggregates in cortex and hippocampus of tTA/TDP-ΔNLS mice. IHC of cortex from tTA/TDP-ΔNLS4 (**A**) and tTA/TDP-ΔNLS19 mice (**B**) at 1 month off Dox with p409/410 TDP-43 antibody shows relatively few aggregates in tTA/TDP-ΔNLS4 mice and higher number of inclusions in tTA/TDP-ΔNLS19 mice. Inclusions in the DG (**C**–**E**) and cortex (**F**–**H**) of tTA/TDP-ΔNLS19 mice 1 week off DOX were immunopositive for p409/410 TDP-43 (**C** and **F**), p403/404 TDP-43 (**D** and **G**), and ubiquitin (Ub) (**E** and **H**) antibodies. (**I**–**N**) Colocalization of pathologic epitopes in TDP-43 aggregates. IF staining with antibodies to ubiquitin (green) and p409/410 TDP-43 (red) demonstrated extensive colocalization within pathological cytoplasmic aggregates (arrows) in cortex (**I**–**N**) from tTA/TDP-ΔNLS19 mice 1 week off Dox. Scale bars: 50 μm (**A** and **B**); 20 μm (**C**–**E**).

ing from neurons showing strong staining to those with negligible staining. This variability was corroborated with an antibody that detects both hTDP-43 and mTDP-43 (h+mTDP-43), as seen by comparing nTg in Figure 2I with hTDP-43-WT in Figure 2, J–L. The number of hTDP-43–expressing neocortical neurons appeared to increase with time off Dox so that approximately 50% of neurons expressed hTDP-43 by 3 months (see Supplemental Figure 7A). Notably, in all of the tTA/TDP-WT lines examined, only extremely rare TDP-43 inclusions were identified in cortical and hippocampal neurons (<0.1% of neurons; see Supplemental Figure 2B) using antibodies that recognize phosphorylated TDP-43 at Ser409 and 410 (p409/410) or ubiquitin. TDP-43 inclusions were not seen in nTg and single tetO-TDP-WT mice. Thus, hTDP-43-WT expression leads to dose- and time-dependent neuron loss in association with gliosis, cerebral atrophy, and rare TDP-43 aggregates.

Cytoplasmic TDP-43 expression leads to progressive neuron loss in tTA/TDP-ΔNLS mice. To evaluate the effects of TDP-43-ΔNLS overexpression in the cytoplasm, we assessed tTA/TDP-ΔNLS4 mice to determine whether neuron loss also occurred with time. Although DG neurodegeneration was variable 1 week after Dox removal, mice sacrificed later displayed increasing levels of neurodegeneration (Figure 3, A–D). Quantitative analyses indicated more acute neuron loss in ΔNLS4 mice such that approximately 50% of the DG neurons were gone at 1 month after induction (Figure 3K).

Consistent with the prominent degeneration of neurons in both tTA/TDP-ΔNLS lines, IHC for GFAP and Iba-1 demonstrated massive gliosis in cortical and hippocampal regions, while areas of low transgene expression (i.e., cerebellum, spinal cord) with no evidence of neuron loss showed no gliosis (Supplemental Figure 3B and data not shown). Selective vulnerability of particular brain regions such as the DG and the deep neocortical layers was observed, while other regions with similar transgene expression such as the hippocampal CA1 subfield and the olfactory bulb were relatively resistant to neurodegeneration (Supplemental Figure 4). Further, IHC studies demonstrated cytoplasmic localization of hTDP-43-ΔNLS in most neurons (70%–90%) of the hippocampus (Figure 3, E–J) and cortex (Supplemental Figure 3A), although some hTDP-43 nuclear staining was observed (see also Supplemental Figure 7A). To better quantify the distribution of exogenous hTDP-43-ΔNLS protein, cortical extracts were separated into enriched nuclear and cytoplasmic fractions and immunoblotted for hTDP-43 and h+mTDP-43 (Figure 3L). Control monogenic tTA mice showed no exogenous hTDP-43 protein in either fraction, whereas endogenous mTDP-43 was predominantly nuclear. In contrast, in tTA/TDP-ΔNLS mice, exogenous protein was found in both nuclear and cytoplasmic fractions, indicating that the ΔNLS mutations were effective in misdirecting TDP-43 to the cytoplasm in concordance with the above IHC results. These find-

Figure 5

Motor dysfunction and CST degeneration in tTA/TDP mice. (**A**) Prevalence of abnormal limb-clasping motor phenotype. tTA/TDP-ΔNLS4 mice showed an early and time-dependent increase in abnormal clasping behavior, with all mice showing motor impairment within 3 weeks off Dox. A lower proportion of tTA/hTDP-WT mice (aggregate data for all WT lines) showed motor impairment only after several months off Dox. This clasping behavior corresponds to spasticity that occurs in PLS and ALS. (**B**) Axonal loss and gliosis of the CST after 1 month off Dox. IHC analysis of the cervical spinal cord using antibodies against phosphorylated NF-H (top row: RMO217) and phosphorylated NF-H+M (second row: TA51) showed loss of axons in the CST (ventral portion of the dorsal columns, top rows). Higher-power view of this region stained with a rabbit anti-NFL antibody in nTg mice showed numerous puncta corresponding to axons in cross-section, which is reduced in tTA/TDP-ΔNLS4 mice (third row). GFAP IHC demonstrated moderate gliosis in tTA-TDP-WT (both WT5 and WT12) and severe gliosis in tTA/hTDP-ΔNLS4 mice. H&E sections of the proximal and distal forelimb and hind limb showed no evidence of atrophy or grouping. Representative sections of biceps are shown. Scale bars: 100 μm (top 2 rows); 10 μm (third row); 50 μm (bottom 2 rows).

ings demonstrated that overexpression of a ΔNLS mutant form of TDP-43 leads to cytoplasmic and nuclear TDP-43, neuron death, and gliosis in the hippocampus and cortex. The somewhat faster rate of neurodegeneration in tTA/TDP-ΔNLS mice relative to tTA/TDP-WT mice appeared to be due to the more widespread, uniform expression pattern of TDP-43-ΔNLS protein compared with the mosaic expression pattern of hTDP-43-WT.

Hyperphosphorylated and ubiquitinated hTDP-43 aggregates in tTA/TDP-ΔNLS mice. To investigate whether the overexpression of hTDP-43-ΔNLS leads to the accumulation of hyperphosphorylated, ubiquitinated cytoplasmic aggregates similar to human TDP-43 proteinopathies (2, 24, 25), IHC was performed using antibodies to phosphorylated epitopes p409/410 and p403/404 of TDP-43 and ubiquitin as markers of pathologically modified TDP-43. Analysis of tTA/TDP-ΔNLS4 mice showed very rare TDP-43 aggregates in less than 1% of cortical neurons, which peaked at 1 month off Dox (Figure 4A). Aggregates in other brain regions, such as the hippocampus and striatum, also were rare to absent (<0.1% of

neurons). In contrast, higher-expressing tTA/TDP-ΔNLS19 mice exhibited slightly more cytoplasmic aggregates in hippocampus (Figure 4, C–E) and cortex (Figure 4, B and F–H). These aggregates peaked at 1 week and 1 month off Dox for the hippocampus and neocortex, respectively, and decreased thereafter. No pathological aggregates were detected in nTg and single tetO-TDP-ΔNLS mice, or in cerebellum or brainstem of ΔNLS4 and ΔNLS19 mice (data not shown). Double-label immunofluorescence (IF) (Figure 4, I–N) using antibodies to p409/410 and ubiquitin demonstrated extensive colocalization in cytoplasmic TDP-43 aggregates. Hence, cytoplasmic expression of hTDP-43 triggers variable accumulation of hTDP-43-ΔNLS aggregates that are hyperphosphorylated and ubiquitinated. However, the paucity of aggregates in tTA/TDP43-ΔNLS4 mice indicated that cytoplasmic inclusions were not required for neuron death.

Clasping motoric phenotype and CST degeneration in tTA/TDP-ΔNLS mice. Previous studies showed that the overexpression of hTDP-43-WT and mutants associated with ALS in spinal cord motor neu-
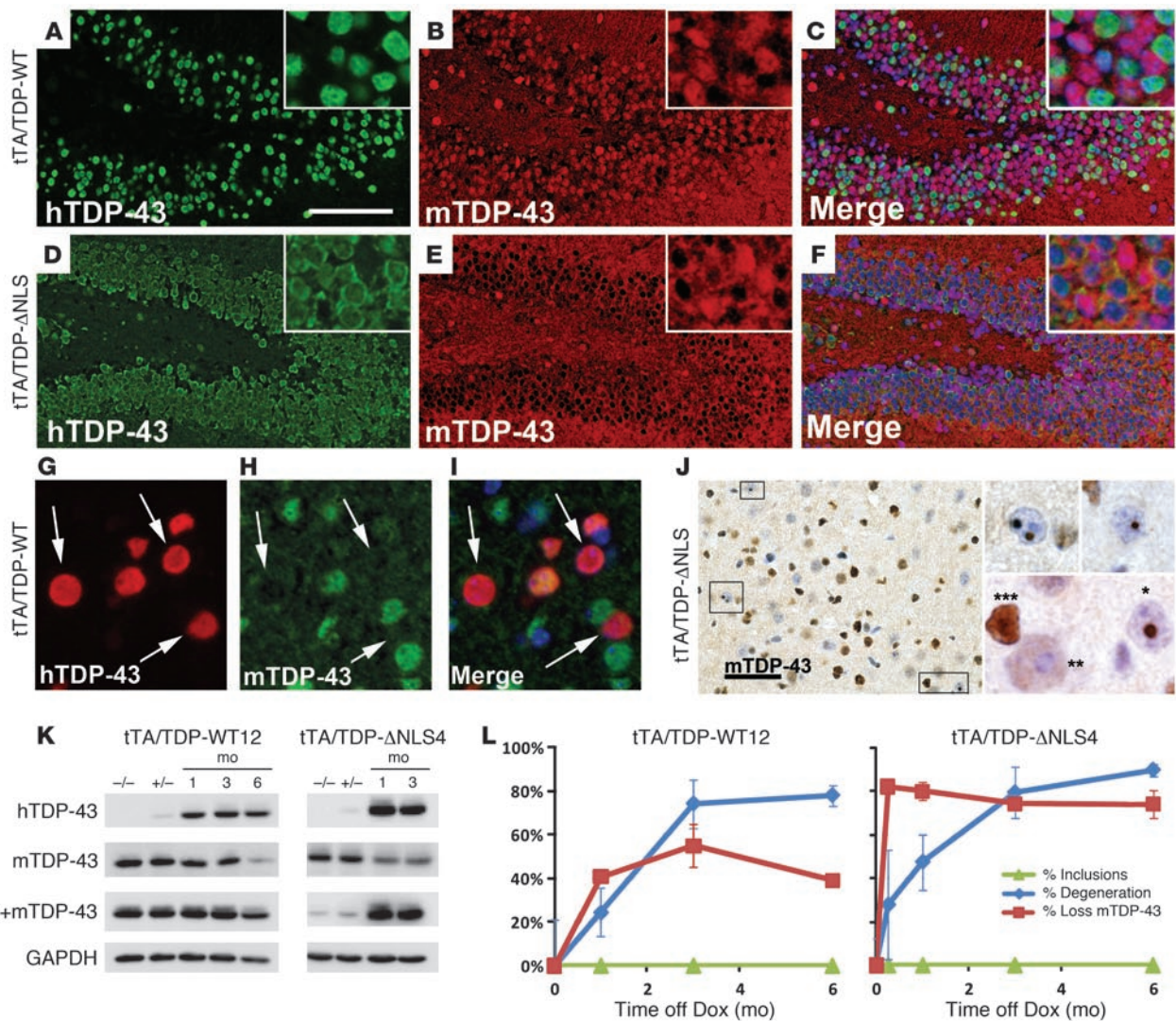
Figure 6
Downregulation of endogenous nuclear mTDP-43 in neurons overexpressing cytoplasmic or nuclear hTDP-43. (**A–I**) hTDP-43 downregulates mTDP-43. IF for hTDP-43 (green) or mTDP-43 (red) in DG of tTA/TDP-WT12 (**A–C**) or tTA/TDP-ΔNLS4 (**D–F**) 1 month off Dox showed neurons expressing hTDP-43 with loss of mTDP-43 staining (insets: higher magnification). (**G–I**) IF for hTDP-43 (red) or mTDP-43 (green) of cortex from tTA/TDP-WT12 mice 1 month off Dox showed loss of mTDP-43 expression in neurons expressing hTDP-43 (arrows). (**J**) Intranuclear mTDP-43 aggregates. IHC of tTA/TDP-ΔNLS19 cortex for mTDP-43 showed rare intranuclear aggregates (insets: higher magnification of boxed regions). Note the absence of mTDP-43 in neurons with aggregates (*) compared with a cell with reduced (**) or normal (***) mTDP-43 expression. Scale bars: 200 μm (**A–F**); 20 μm (**G–I**); 50 μm (**J**). (**K**) Reduced mTDP-43 protein in tTA/TDP mice. Immunoblot for hTDP-43, mTDP-43, and h+mTDP-43 of cortical RIPA extracts from tTA/TDP-WT12 or tTA/TDP-ΔNLS4 at various times off Dox showed increased hTDP-43 and reduced mTDP-43 protein relative to nTg (–/–) and tetO-TDP monogenic (+/–) mice. GAPDH is a loading control. (**L**) Quantification of immunostained sections of DG from tTA/TDP-WT12, tTA/TDP-ΔNLS4 mice, and control nTg and monogenic (tTA only or tetO-TDP only) mice (*n* = 29). The percentage of neurons with inclusions (green, p409/410 stained sections), percentage of neurons with reduced mTDP-43 expression (red, anti-mTDP43 stained sections) and percentage of neuronal degeneration (blue, H&E sections as in Figures 2 and 3) are shown as mean ± SEM versus time off Dox (*t* = 0 represents control mice).

rons led to motor impairments (16–20). Since the Camk2a promoter does not direct hTDP-43 expression in spinal cord motor neurons (see Figure 1), we asked whether hTDP-43-ΔNLS expression in motor cortex is sufficient to cause motor impairments. Abnormal "clasping" is a measure of spastic motor impairment (26–28), and the tTA/TDP-ΔNLS mice displayed abnormal limb clasping as early as 1 week after induction and throughout their life spans until sacrifice at 6 months after induction (Figure 5A).

In contrast, the tTA/TDP-WT mice showed less robust and more variable clasping, which was detected only after approximately 1–3 months after induction (Figure 5A). No clasping phenotype was observed in nTg or single Tg littermates.

To determine whether upper motor neuron pathology is responsible for this motoric phenotype, sections of brain, spinal cord, and skeletal muscle were examined for evidence of degeneration. Gliosis was noted at all levels of the CST in tTA/TDP-ΔNLS mice,
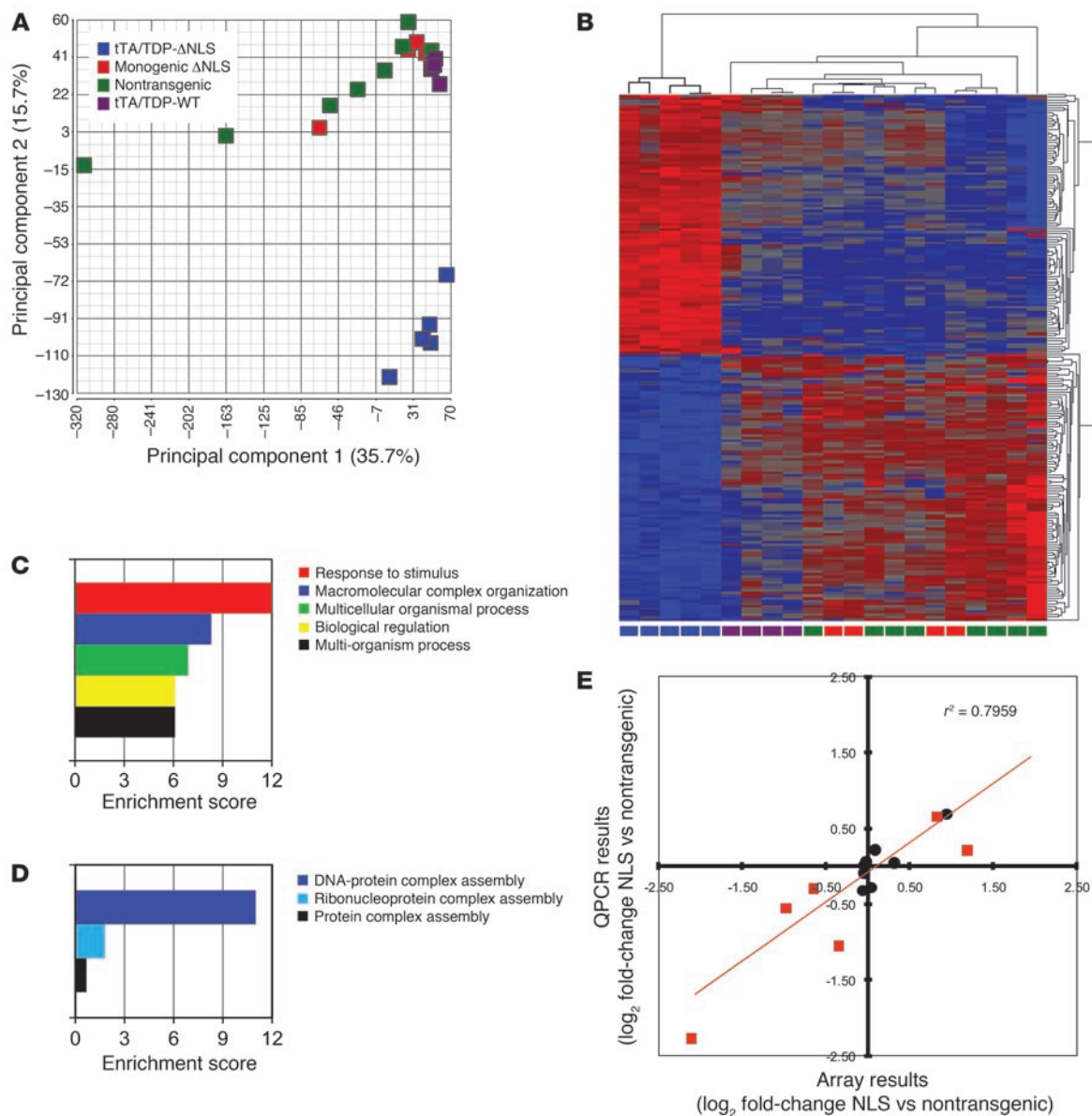
Figure 7
Analysis of global mRNA expression. (**A**) Principal component (PC) analysis revealed a distinct global gene expression signature for tTA/TDP-ΔNLS (tTA/TDP-ΔNLS4, blue, $n = 5$), while other groups (nTg $n = 8$, tTA/TDP-WT $n = 4$, and monogenic ΔNLS $n = 4$) were relatively admixed. Data shown as PC1 versus PC2 for each individual mouse. (**B**) Hierarchical cluster analysis of the genes differentially expressed between tTA/TDP-ΔNLS and nTg mice (FDR < 0.05, with absolute value of FC > 2, shown here, $n = 197$ genes) corroborated PC analysis. Genes dysregulated in tTA/TDP-ΔNLS mice were evenly split between those downregulated (blue) and upregulated (red). Columns on heat map correspond to individual animals designated as follows: tTA/TDP-ΔNLS (blue), nTg (green), tTA/TDP-WT (purple), and monogenic ΔNLS (red). Rows correspond to individual probe sets, with blue indicating lower, gray indicating intermediate, and red indicating higher expression. (**C**) Biological pathway analysis of genes dysregulated in tTA/TDP-ΔNLS mice revealed many enriched pathways. The top 5 enrichment scores (negative $\log_{10} \chi^2$ P value) are shown (higher score indicates greater enrichment). (**D**) Within the second-most-enriched pathway (macromolecular complex assembly, blue bar in **C**), most of the genes were involved in DNA-protein complex assembly. (**E**) Microarray and qRT-PCR results showed good concordance (r^2 of 0.7959, and no discordant directions of change), as shown by plotting $\log_2$ FC values for microarray data (x axis) versus qRT-PCR results (y axis). The 6 genes that differed significantly between tTA/TDP-ΔNLS and nTg littermates (red squares) and 8 genes that did not differ significantly between groups (black circles) are shown (see Table 2). A negative value denotes lower expression in the tTA/TDP-ΔNLS mice.

including the striatum, cerebral peduncles, medullary pyramids, and cervical spinal cord (Supplemental Figure 5). Using antibodies to phosphorylated and phosphorylation-independent neurofilament (NF) subunits as axonal markers, we observed select loss

of CST axons in cervical spinal cord associated with gliosis (Figure 5B). Lower motor neuron loss was not observed, consistent with the absence of gliosis of the spinal cord ventral horn, and the absence of grouped atrophy or other abnormalities of the proximal

Table 1

Top 10 genes in the DNA-protein complex assembly pathway

Gene name	P value	FC
Nucleosome assembly protein 1-like 1	5.78×10^{-11}	−1.2504
Nucleosome assembly protein 1-like 1/ predicted gene 4204	2.61×10^{-09}	−1.2624
Histone cluster 1, H2bp	1.13×10^{-08}	1.8277
Histone cluster 1, H4a/H4b/H4c	1.41×10^{-08}	1.8690
Prion protein	1.41×10^{-08}	1.2641
Histone cluster 1, H3d	1.55×10^{-07}	2.2811
Nucleosome assembly protein 1-like 2	1.84×10^{-07}	−1.4639
Olfactomedin 1	4.64×10^{-07}	−1.1636
Histone cluster 1, H4h	5.09×10^{-07}	2.3303
Nucleosome assembly protein 1-like 1	1.18×10^{-06}	−1.2576

Genes were ordered by smallest nominal P value comparing tTA/TDP-ΔNLS mice relative to nTg littermates.

and distal forelimb and hind limb striated muscles (Figure 5B). Thus, our findings support that degeneration of motor neurons in the cortex is sufficient to elicit a motoric phenotype reminiscent of both FTLD-TDP and PLS due to the selective involvement of upper but not lower motor neurons.

Nuclear or cytoplasmic overexpression of hTDP-43 leads to downregulation of endogenous mTDP-43. Since the profound neurodegeneration in tTA/TDP-ΔNLS mice could not be accounted for by rare cytoplasmic TDP-43 inclusions and since previous studies have shown that hTDP-43-WT or hTDP-43-ΔNLS expression reduces endogenous mTDP-43 levels in cultured nonneuronal cells (11), we asked whether overexpression of hTDP-43 decreases endogenous mTDP-43. To this end, we developed what we believe is a novel mouse-specific TDP-43 polyclonal antibody raised to a synthetic peptide corresponding to residues 203–219 of mTDP-43 (only 58% sequence identity with hTDP-43). Triple-affinity purification of the polyclonal antisera showed that it reacted specifically with mTDP-43 and not hTDP-43 by immunoblot and by IHC analyses (Supplemental Figure 6). Double-label IF using antibodies specific for hTDP-43 and mTDP-43 showed the absence or a reduction of endogenous mTDP-43 in neurons that expressed hTDP-43 in both tTA/TDP-WT (Figure 6, A–C) and tTA/TDP-ΔNLS (Figure 6, D–F) mice. Indeed, higher-power images showed that neurons expressing exogenous hTDP-43 protein exhibited reduced immunostaining of endogenous mTDP-43 (Figure 6, G–I). Interestingly, since tTA/TDP-ΔNLS mice show more uniform transgene expression, greater numbers of DG neurons were devoid of mTDP-43 expression, in contrast with the mosaic expression of hTDP-43-WT and the concomitant mosaic reduction of mTDP-43 in tTA/TDP-WT mice (compare Figure 6, A–C with D–F). Notably, neurodegeneration was only seen in regions in which there was a reduction of nuclear mTDP-43 staining. Regions with low or no transgene expression or neurodegeneration, such as the ventral motor neuron pool in spinal cord, showed no change in endogenous nuclear mTDP-43 staining (data not shown). Interestingly, very rare cells with mTDP-43 nuclear inclusions were identified (Figure 6J). Significantly, we also did not observe sequestration of endogenous mTDP-43 into hTDP-43 inclusions in our hTDP-43 Tg mice.

The reduction of endogenous mTDP-43 secondary to exogenous hTDP-43 expression was confirmed by immunoblotting. Endogenous mTDP-43 protein was decreased in tTA/TDP-WT12 mice at

6 months off Dox, whereas mTDP-43 protein was reduced as early as 1 month off Dox in tTA/hTDP-ΔNLS4 mice (Figure 6K). The delayed biochemical detection of mTDP-43 reduction was consistent with the slower onset and mosaic expression pattern of tTA/TDP-WT12 mice. To confirm that endogenous nuclear TDP-43 protein was reduced in Tg mice, immunoblotting of nuclear versus cytoplasmic enriched fractions was performed, which showed that in control mice, endogenous mTDP-43 is detected only in nuclear enriched fractions and that nuclear mTDP-43 protein levels are reduced in tTA/TDP-ΔNLS4 mice (Figure 3L). Given the neuronal specificity of the Camk2a promoter, the decrease in mTDP-43 protein levels in whole cortical lysates is indicative of a marked reduction of mTDP-43 protein in affected cells.

To examine the relationship among neurodegeneration, TDP-43 aggregates, and the downregulation of endogenous mTDP-43, quantification of percentage of neuron loss, percentage of neurons with TDP-43 aggregates, and percentage neurons with reduced mTDP-43 protein was performed (Figure 6L). TDP-43 aggregates in DG were extremely rare at all time points and therefore bear no relationship with neuron loss. In contrast, the reduction in mTDP-43 protein appeared to correlate with the extent of neurodegeneration. Significantly, more rapid degeneration in tTA/TDP-ΔNLS mice compared with tTA/TDP-WT mice was matched with more uniform and rapid loss of mTDP-43 protein. Moreover, the number of neurons with loss of mTDP-43 protein decreased relative to the number of unaffected neurons as a function of time off Dox, suggesting that neurons with reduced mTDP-43 protein are selectively vulnerable. Hence, these data indicate that overexpression of hTDP-43 leads to a downregulation of endogenous nuclear mTDP-43 expression, which correlates with the rate and extent of neurodegeneration, suggesting that dysregulation of endogenous TDP-43 activity may be linked to neuron death.

tTA/TDP-ΔNLS mice demonstrate substantial alterations in gene expression, particularly affecting chromatin assembly pathways. Thus far, our data suggest that endogenous mTDP-43 expression is strongly affected by exogenous hTDP-43 expression. Presumably, this tight regulation is required for the normal physiologic functions of endogenous TDP-43. To better understand the consequences of these observed changes, in particular the genome-wide effects of expressing hTDP-43-ΔNLS and perturbing mTDP-43, we used microarrays to evaluate global gene expression in the cortices of tTA/TDP-ΔNLS and tTA/TDP-WT animals relative to single Tg mice and nTg littermates. The inducible system allows analysis of relatively rapid changes in gene expression to avoid unrelated developmental effects and before secondary reactive changes due to neurodegeneration confound our analysis. Mice were studied at 2 weeks off Dox, a time point when tTA/TDP-ΔNLS mice showed uniform hTDP-43 expression and widespread reduction in mTDP-43, but prior to onset of significant gliosis and massive cell loss. It is worth noting that the widespread hTDP-43 expression observed in tTA/TDP-ΔNLS mice at this 2-week time point stands in contrast with tTA/TDP-WT mice, which showed mosaic hTDP-43 expression in less than 10% of neurons (Supplemental Figure 7A). The differing levels of transgene expression in the tTA/TDP-ΔNLS and tTA/TDP-WT mice were corroborated by both hTDP-43 mRNA (Supplemental Figure 7B) and protein levels (Supplemental Figure 7C), which showed robust hTDP-43 expression in tTA/TDP-ΔNLS mice relative to tTA/TDP-WT mice at early time points after Dox removal.

In cortical samples from tTA/TDP-ΔNLS4 (at 2 weeks when there is minimal confounding changes due to gliosis and neuron loss),

Table 2
qRT-PCR verification of microarray results

Gene name	Symbol	*P* value		log$_2$ FC	
		Array	qRT-PCR	Array	qRT-PCR
Sperm associated antigen 5	*Spag5*	0.00000	0.00002	−2.10	−2.27
NF, light polypeptide	*Nefl*	0.00023	0.00008	−0.35	−1.05
TAR DNA–binding protein 43	*Tardbp*	0.00000	0.00001	−0.98	−0.55
Heterogeneous ribonucleoprotein A3	*Hnrnpa3*	0.00000	0.00646	−0.64	−0.30
Histone cluster 1, H3d	*Hist1h3d*	0.00000	0.00489	1.19	0.21
Antisilencing function 1 homolog A	*Asf1a*	0.00000	0.00002	0.83	0.66
Cyclin-dependent kinase 6	*Cdk6*	0.34964	0.00895	−0.06	−0.32
Microtubule-associated protein 2	*Mtap2*	0.82589	0.03381	0.04	−0.28
Histone deacetylase 6	*Hdac6*	0.60055	0.26069	−0.04	−0.09
CD34 antigen	*Cd34*	0.72897	0.47809	−0.04	0.01
Glial fibrillary acid protein	*Gfap*	0.18572	0.37695	0.32	0.04
NF, medium polypeptide	*Nefm*	0.69349	0.34692	−0.02	0.06
Granulin	*Grn*	0.53551	0.06419	0.09	0.22
Glutamate receptor, ionotropic, NMDA1 (zeta 1)	*Grin1*	0.07654	0.00003	0.95	0.69

Gene expression assessed by microarray and qRT-PCR for 14 selected genes. *P* values and log$_2$ FC relative to nTg mice are shown, with negative FC values denoting lower expression in the tTA/TDP-ΔNLS mice.

all the tTA/TDP-ΔNLS animals (*n* = 5), regardless of sex, showed a dramatically different global gene expression profile compared with the other mouse lines (Figure 7, A and B). In all, more than 4,700 genes were differentially expressed between tTA/TDP-ΔNLS and nTg mice (false discovery rate [FDR] < 0.05), with 197 showing fold change (FC) differences greater than 2. Differentially expressed genes were evenly distributed between those increased versus decreased in tTA/TDP-ΔNLS mice (Figure 7B), making it unlikely that neuron loss alone could account for these findings. Biological pathway analysis of differentially expressed genes further revealed a number of dysregulated pathways (Figure 7C), with the relatively nonspecific category "response to stimulus" showing the greatest enrichment in dysregulated genes, followed by the category "macromolecular complex organization," with a highly significant enrichment score of 8.3, corresponding to a *P* value of less than 10^{-8}. Within this category, genes involved in chromatin assembly accounted for the significant enrichment of the entire category (Figure 7D), with 4 of the top 10 genes in this category coding for histones (Table 1). Remarkably, all 4 histone genes were upregulated in the tTA/TDP-ΔNLS mice.

In contrast with the tTA/TDP-ΔNLS animals, the tTA/TDP-WT mice (*n* = 4), which express much lower levels of transgene and have correspondingly less repression of endogenous mTDP-43, showed more modest changes in global gene expression (Figure 7A). While these animals did separate from nTg mice, their global gene expression signature appeared to be intermediate between the nTg and tTA/TDP-ΔNLS mice (Figure 7, A and B).

To validate our microarray findings as well as interrogate the expression of genes previously reported to be affected by TDP-43, we performed quantitative RT-PCR (qRT-PCR) on select genes. As shown in Figure 7E, microarray and qRT-PCR results were concordant (*r*^{2} of 0.7959 across 14 genes tested on both platforms). Of note, while some genes previously reported to be affected by TDP-43 (e.g., *Nefl*) were dysregulated in both our microarray and qRT-PCR experiments, this was not true for other genes reported to be transcriptionally affected by TDP-43 (e.g., *Hdac6* and *Cdk6*) (29–31). In addition, the mouse *Tardbp* gene itself is downregulated by log$_2$ FC

of −0.55 (32% reduction) by qRT-PCR in tTA/TDP-ΔNLS mice relative to nTg littermates (Table 2). This finding is concordant with our IF and immunoblot studies demonstrating that endogenous mTDP-43 is downregulated in the presence of exogenous hTDP-43 and implies that at least part of this regulatory effect occurs at the mRNA level. Significantly, we noted that mRNA markers of astrocytes (*Gfap*), microglia (*Cd34*), and neurons (*Nefm*) did not differ substantially between the tTA/TDP-ΔNLS mice and their nTg littermates, thereby indicating that gliosis, microglial infiltration, and neuron loss were not responsible for the gene expression changes seen here.

Taken together, these data indicate that tTA/TDP-ΔNLS mice show significantly altered global gene expression affecting specific pathways such as chromatin assembly. Although tTA/TDP-WT mice showed a somewhat intermediate profile, their pattern of gene expression was closer to that of nTg mice, presumably due to their mosaic hTDP-43 expression pattern affecting only a small subset of neurons at the time point studied. Regardless, specific biological pathways, in particular those involved in chromatin assembly, were linked to the dysregulation of endogenous TDP-43 and downstream neurodegeneration.

Discussion

TDP-43 is a multifunctional DNA- and RNA-binding protein expressed mainly in the nucleus of nearly all cells, but abnormal forms of TDP-43 aggregate mostly as cytoplasmic inclusions in FTLD-TDP and ALS. It is unclear whether the mechanisms of disease pathogenesis are due to loss of normal TDP-43 function or a gain of toxic function linked to aggregate formation or accumulation of TDP-43 CTFs. Furthermore, the relative roles of mislocalization, abnormal expression, abnormal downregulation, or aggregation of TDP-43 in causing neurotoxicity are not known. To address these questions, we generated Tg mice selectively expressing hTDP-43-ΔNLS in forebrain neurons and compared them with hTDP-43-WT–expressing Tg mice using the Camk2a tet-O inducible system. Remarkably, we found that endogenous mTDP-43 is tightly regulated and that expression of hTDP-43-ΔNLS or TDP-43-WT leads to a reduction of nuclear mTDP-43 in vulnerable neurons with associated neuron death, thereby implicating the dysregulation of nuclear TDP-43 expression and the loss of nuclear TDP-43 functions in the pathogenesis of TDP-43 proteinopathies.

The regional expression pattern of hTDP-43 in our Tg mouse models followed that of Camk2a promoter and was accompanied by the selective degeneration of hippocampal DG neurons, neocortical neurons (including the axons of upper motor neurons), and the CST emanating from upper motor neurons with sparing of spinal cord motor neurons. Thus, these Tg mice, especially tTA/TDP-ΔNLS mice, recapitulate key aspects of FTLD-TDP and PLS including (a) progressive and targeted neurodegeneration, (b) dys-

regulation and loss of endogenous TDP-43, and (c) presence, albeit rare, of phosphorylated and ubiquitinated TDP-43 inclusions in affected neurons. Moreover, the observed spastic motor phenotype is likely due to selective degeneration of axons in the CST that emanate from upper motor neurons without TDP-43 pathology in or degeneration of spinal cord motor neurons in tTA/TDP-ΔNLS mice. Thus, our results suggest that it is possible to model a PLS-like phenotype in Tg mice where TDP-43 dysfunction affects motor cortex without subsequent lower motor neuron degeneration.

Both tTA/TDP-ΔNLS and tTA/TDP-WT mice showed time-dependent neurodegeneration. However, only the highest expressing tTA/TDP-ΔNLS19 mice showed significant, but very small numbers of TDP-43 aggregates, while tTA/TDP-ΔNLS4 and all tTA/TDP-WT lines showed vanishingly few TDP-43 aggregates, suggesting that inclusions may not be necessary for neurodegeneration. Instead, neuron loss may result from perturbations of endogenous mTDP-43. Supporting such an argument are studies demonstrating that endogenous TDP-43 expression is tightly regulated and is critical for survival. For example, knockout of *Tardbp* in mice led to embryonic lethality (12–15), heterozygous knockout mice develop motor impairments with age (12), and conditional knockout mice exhibit rapid postnatal lethality (15). Further, downregulation of TDP-43 in differentiated Neuro-2a cells inhibits neurite outgrowth and induces cell death (32). These studies indicate that perturbation of normal TDP-43 function is detrimental.

Although WT or mutant human or mouse TDP-43 expression in *Drosophila* or Tg mice has been shown to cause neurotoxicity, the exact cause of neurodegeneration in these models is unknown (16–20, 33). Our mice are similar to previously reported Tg mice in that we observe selective vulnerability of neuronal populations including upper motor neurons, a motor phenotype, and the variable presence of TDP-43 aggregates (16–20). These previously reported Tg mouse models implicate pathological aggregates, high levels of insoluble TDP-43, and measurable levels of TDP-43 CTFs as likely causes of neurodegeneration. However, the low levels (<10%) of insoluble TDP-43 and the absence of CTFs with only rare TDP-43 inclusions in our tTA/TDP-ΔNLS and tTA/TDP-WT mice make it unlikely that insoluble hTDP-43 aggregates are directly responsible for neuron loss in our Tg mice. Indeed, varying levels of detergent-soluble CTFs have been detected in brain lysates of other Tg lines (16–20). However, we observed a very similar neurodegeneration phenotype compared with these other models, indicating that CTFs are not a requisite for neurodegeneration. Although we cannot exclude a toxic gain of function due to overexpressed hTDP-43, our demonstration that hTDP-43 expression leads to downregulation of endogenous mTDP-43 mRNA and protein in neurons, which correlates with neuron death, suggests that the dysregulation of normal mTDP-43 expression and thus disruption of normal mTDP-43 function may be a major contributor to neurodegeneration.

Notably, we demonstrated direct "replacement" of mTDP-43 by exogenous hTDP-43 in both the tTA/TDP-WT and tTA/TDP-ΔNLS models by generating what we believe is a novel antibody specific to endogenous mTDP-43. The availability of species-specific antibodies to endogenous mTDP-43 and exogenous hTDP-43 allows us to conduct quantitative IHC in our Tg mice to determine the temporal relation of mTDP-43 and hTDP-43 neuronal expression at various time points off Dox in our Tg mice. We found that neuron death was linked to loss of mTDP-43 protein and not to the number of TDP-43 aggregates. Thus, the perturbation of endogenous mTDP-43 by the overexpression of hTDP-43 appears sufficient to

cause neuron loss, perhaps due to the inability of hTDP-43 ortholog to replace the function of mTDP-43 or because perturbation of the tight regulation of TDP-43 leads to aberrant TDP-43 function, thereby resulting in neurodegeneration. Other Tg models have shown that neurons bearing TDP-43 inclusions exhibit absence of nuclear TDP-43 protein by IHC, similar to that seen in human disease tissue (16–18). Furthermore, we and others have shown that exogenous TDP-43 protein expression downregulates endogenous TDP-43 expression in cell or tissue homogenates (11, 20). Our current results are unique in that we link "nuclear clearing" and the dysregulation of endogenous TDP-43 expression and show that the regulation of TDP-43 expression occurs on the cellular level in neurons expressing hTDP-43 even in the absence of TDP-43 inclusions. This was the major correlate to neuron death, suggesting that dysregulation of TDP-43 expression is linked to neurodegeneration.

Since the pathways by which TDP-43 dysregulation leads to neurodegeneration are not entirely known, it is difficult to be certain that hTDP-43 overexpression is unable to compensate for the loss of mTDP-43 expression. However, we note that the stabilization of *Nefl* mRNA is the only neuron-specific effect of TDP-43 protein that is currently known (31). Consistent with a loss of TDP-43 function in neurons, we observed a specific reduction in *Nefl* expression in Tg mice, while expression of *Nefm* and *Nefh* were unchanged. Moreover, a recent study overexpressing WT mTDP-43 in Tg mice using a Camk2a promoter (16) showed similar neurodegeneration as the overexpression of hTDP-43. Therefore, an important determinant of neurotoxicity may be the dysregulation of TDP-43 expression.

The mechanism whereby both exogenous hTDP-43-ΔNLS and hTDP-43-WT results in a reduction in mTDP-43 expression is not known. However, since we observed high levels of the TDP-43-ΔNLS protein in the nucleus, the most parsimonious explanation for neurodegeneration in our Tg mice is that elevated levels of nuclear hTDP-43 protein result in downregulation of endogenous mTDP-43 mRNA and nuclear mTDP-43 protein levels. However, since TDP-43-ΔNLS protein is also localized to the cytoplasm in our mice, we cannot entirely exclude the possibility that cytoplasmic TDP-43 plays a role in the reduction of endogenous TDP-43 or has a direct neurotoxic effect. Nonetheless, since downregulation of endogenous nuclear mTDP-43 was observed in both hTDP-43-WT and hTDP-43-ΔNLS mice, it is plausible that perturbation of nuclear TDP-43 protein levels leads to dysregulation of endogenous mTDP-43 expression, which culminates in neuron death.

Our tTA/TDP-ΔNLS mice provide unique opportunities to study global changes in gene expression mediated by TDP-43. This is because of the synchronized inducible overexpression of TDP-43-ΔNLS in approximately 80% of the neurons and the identification of a window of opportunity at 2 weeks off Dox where transgene was expressed and endogenous mTDP-43 protein was reduced, and secondary reactive changes such as gliosis in response to neurodegeneration were at a minimum. Such profound changes in gene expression were not detected in tTA/TDP-WT mice, likely due to the low percentage of neurons (~10%) expressing transgene and nearly normal endogenous mTDP-43 expression in tTA/TDP-WT mice at 2 weeks off Dox. The reason for nonsynchronized transgene expression in tTA/TDP-WT mice is not known, but 3 of the 4 lines of tTA/TDP-WT mice reported here showed this phenotype. Thus, we infer that the profound changes in global gene expression observed in tTA/TDP-ΔNLS but not in the tTA/TDP-WT mice reflect the uniform loss of endogenous mTDP-43. Although these findings clearly require further studies of TDP-43–knockout

or –knockdown models, our data prompt us to hypothesize that these changes in gene expression result from a loss of function of normal nuclear TDP-43. In summary, the behavioral, biochemical, IHC, and molecular analyses of these inducible hTDP-43 Tg mice advance our understanding of the biology of TDP-43, in particular, with regards to the tight regulation of TDP-43 expression, thereby underscoring the integral role of TDP-43 expression in gene regulation and neurodegeneration pathways.

Methods

Generation of hTDP-43-WT and -ΔNLS transgenic mice. hTDP-43 Tg lines were generated by injection of linearized moPrP-tetP vector containing hTDP-43-WT and hTDP-43-ΔNLS cDNA (11) into pronucleus of fertilized eggs from C57BL/6J × C3HeJ F1 matings (34). Monogenic tetO-TDP-WT and tetO-TDP-ΔNLS mice were bred to Camk2a-tTA mice (Jackson Laboratory) generating nTg, tTA monogenic, single tetO-TDP-43 Tg mice, and bigenic mice expressing hTDP-43-WT or hTDP-43-ΔNLS (Figure 1A). Breeding mice and pups were fed chow containing 200 mg/kg Dox (Dox Diet, S3888; Bio-Serv). Mice were switched to standard chow (Lab Diet 5053, Test Diet; PMI International) to induce hTDP-43 expression (Figure 1B). Genotyping from tail DNA (35) was performed using the following primers: TDP-forward (TTGGTAATAGCAGAGGGGGTGGAG), MoPrP-reverse (TCCCCCAGCCTAGACCACGAGAAT), Camk2a-tTA-forward (CGCTGT-GGGGCATTTTACTTTAG), and Camk2a-tTA-reverse (CATGTCCAGATC-GAAATCGTC). All procedures were performed in accordance with the NIH Guide for the Care and Use of Experimental Animals and approved by the University of Pennsylvania Institutional Animal Care and Use Committee.

Antibodies. Antibodies used in this study were as follows: rabbit anti–TDP-43 polyclonal antibody (pAb) raised to amino acids 1–260 (Proteintech Group), a human specific mouse mAb raised to the same TDP-43 sequence (Proteintech), rabbit anti–phospho-Ser403/Ser404 TDP-43 (Cosmo Bio Co.), rabbit anti-GFAP (DAKO North America), rabbit anti–Iba-1 (Wako Chemicals USA), rabbit anti-ubiquitin (DAKO), anti–α-glyceraldehyde-3-phosphate dehydrogenase (GAPDH 6C5 mouse mAb; Advanced ImmunoChemical Inc.), anti-NF mAbs to phosphorylated epitope on high-Mr NF (pNF-H) subunit and mid- and high-Mr NF (pNF-M+H) subunits as well as a rabbit pAb to the low NF (NF-L) subunit (36), affinity-purified rabbit anti–TDP-43 pAb raised to amino acids 394–414 (h+mTDP-43; ref. 37), and rat phospho-specific mAb that recognizes TDP-43 phosphorylated at Ser409/Ser410 (p409/410; ref. 25). 15A, an affinity-purified pAb specific for mTDP-43, was generated by immunizing rabbits with a synthetic peptide corresponding to residues 203–219 of mTDP-43 (TAEELQQFFCQYGEVVD) and was characterized by immunoblot and IHC (Supplemental Figure 6).

Immunohistochemistry and histological staining. Mice were perfused and tissues were processed for IHC and IF as described (21). In general, the left hemisphere was dissected into cortex, hippocampus, cerebellum, olfactory bulb, and the rest of the tissue (subcortical structures, brainstem) and frozen at –80°C until used for biochemical analysis. The right hemisphere and spinal cord sections were immersed in neutral buffered formalin (NBF) (Fisher Scientific) and processed for IHC (21, 35).

For unbiased estimates of hippocampal DG neuron numbers, H&E coronal sections at the level of the mammillary body were used for quantitative analysis (n = 3–4 per group) as previously described (35). Digital photomicrographs were used to manually count the number of DG granule neurons. For quantification of percentage of neurons with reduced mTDP-43 and the percentage of neurons with TDP-43 aggregates, high-power photomicrographs of the DG from sections immunostained for mTDP-43 or p409/410 were manually counted and the percentage of viable neurons with reduced mTDP-43 staining or containing an inclusion was calculated.

Double-label IF was conducted as previously described (35, 37) using Alexa Fluor 488– and 594–conjugated secondary antibodies (Molecular Probes). Digital images were obtained using an Olympus BX 51 microscope equipped with brightfield and fluorescence light sources using a DP71 digital camera (Olympus) and DP Manager software (Olympus).

SDS-PAGE and immunoblot analysis. Tissues were sequentially extracted first with 5 volumes (ml/g) of RIPA buffer (0.1% SDS, 1% Nonidet P-40, 0.5% sodium deoxycholate, 5 mM EDTA, 150 mM NaCl, 50 mM Tris-HCl, pH 8.0) containing protease and phosphatase inhibitor cocktail. After the insoluble pellets were washed with RIPA buffer, they were further extracted with 2.5 vols of urea buffer (7 M urea, 2 M thiourea, 4% CHAPS, 30 mM Tris-HCl, pH 8.5). 30 μg of RIPA extract or 4× equivalent vols of urea extract per lane were separated on a 10% Tris-glycine SDS-PAGE gel and immunoblotted as described (35). Digital images were acquired using a Fuji Film Intelligent Darkbox II (Fuji Systems). Quantification of band intensity was performed using Image Quant software (Molecular Dynamics). For transgene expression quantification, fold expression relative to nTg and tTA control mice was determined using h+mTDP-43 immunoblots within the linear range of band intensity after normalization to GAPDH expression.

Enriched nuclear and cytoplasmic fractions were prepared from mouse cortex by modified method of Guillemin et al. (38). Briefly, cortex was weighed, placed in hypotonic buffer containing protease inhibitors (10 mM HEPES-KOH, 10 mM KCl, 1.5 mM MgCl₂, pH 7.4; 5:1, v/w) and homogenized using 8 passes of Dounce homogenizer. After incubation for 10 minutes at 4°C, 2.0 M sucrose (1:1, v/w) was added and the suspension further homogenized using 15 passes of Dounce homogenizer; it was then centrifuged at 1000 g for 5 minutes at 4°C. The supernatant was collected. The pellet was resuspended in 10 volume of hypotonic buffer containing 0.3 M sucrose and rehomogenized using 8 strokes of Dounce homogenizer and centrifuged as before. The resultant supernatant was combined with the first as the cytoplasmic fraction. The pellet was washed in hypotonic buffer containing 0.3 M sucrose and centrifuged as before. The final enriched nuclear fraction was resuspended in hypotonic buffer containing 0.3 M sucrose. The fractions were sonicated and processed for SDS-PAGE.

Clasping phenotype. Bigenic and monogenic hTDP-43 Tg mice as well as age-matched control nTg mice were suspended by the tail 30 cm above an open cage for 30 seconds, after which they were slowly lowered toward the bottom of the cage. A positive response was recorded for mice that clasped their limbs within 5 seconds of suspension while maintaining the clasping posture until lowered to the cage.

Brain RNA isolation and microarray/qRT-PCR quantification. Animals from all groups were sacrificed and hippocampi and right cortex were immediately placed into QIAzol reagent (QIAGEN). Samples were homogenized by passing through a series of 3 increasingly higher-gauge needles. After homogenization, total RNA was isolated from the samples by following the protocol for the miRNeasy kit (QIAGEN). RNA was run on an Agilent 2100 Bioanalyzer to assess quality; only samples with excellent RNA quality (RNA Integrity Number [RIN] > 7) were used. For microarray experiments, RNA samples were evaluated on the Affymetrix Mouse Genome 430A 2.0 Array following standard Affymetrix protocols (GEO GSE25182). For qRT-PCR experiments, RNA was reverse transcribed to cDNA using SuperScript III (Invitrogen). qPCR was performed on the cDNA using an Applied Biosystems 7500 Fast Real-Time PCR system using custom-designed primers and Sybr Green. Gene expression values were determined by using the $\Delta\Delta C_T$ method. Human- and mouse-specific TDP-43 primers were designed and tested with control mRNAs to assess lack of interspecies cross-reactivity. The genes of interest were standardized to the geometric mean of 2 housekeeping genes (GAPDH and β-actin). Samples were normalized only within a brain region to a common animal.

Microarray analysis and statistical methods. The Partek Genomics Suite was used to perform microarray data analysis and to generate graphics (Partek

GS). Affymetrix array raw fluorescence intensity measures of gene expression were normalized and quantified using robust multi-array analysis. To identify genes differentially expressed between groups, we employed ANOVA, followed by pairwise contrasts between the groups of interest. Our model corrected for sex. To correct for multiple hypothesis testing, we calculated FDR using the Benjamini-Hochberg method. Principal components analyses and hierarchical cluster analyses (Pearson's correlation coefficient) were employed to evaluate patterns of global gene expression. Differentially expressed genes were additionally subjected to biological pathway analysis using the Gene Ontology database to find pathways enriched in dysregulated genes; enrichment scores are the negative $\log_{10} \chi^2$ P value.

Statistics. Statistical analyses of DG neuron counts, brain weights, and mTDP-43 and hTDP-43 transcripts among nTg, monogenic, and bigenic mouse lines were performed by 1-way ANOVA with Bonferroni's multiple comparison post-hoc test (Prism 4.01; GraphPad Software). $P < 0.05$ was considered significant.

Acknowledgments

Address correspondence to: Virginia M.-Y. Lee, Department of Pathology and Laboratory Medicine, University of Pennsylvania School of Medicine, Maloney 3, HUP, 3600 Spruce Street, Philadelphia, Pennsylvania 19104-4283, USA. Phone: 215.662.6427; Fax: 215.349.5909; E-mail: vmylee@mail.med.upenn.edu.

Lionel M. Igaz's present address is: Departamento de Fisiología y Biofísica, Facultad de Medicina, Universidad de Buenos Aires, Ciudad de Buenos Aires, Argentina.

1. Mackenzie IR, Feldman HH. Ubiquitin immunohistochemistry suggests classic motor neuron disease, motor neuron disease with dementia, and frontotemporal dementia of the motor neuron disease type represent a clinicopathologic spectrum. *J Neuropathol Exp Neurol.* 2005;64(8):730–739.

2. Neumann M, et al. Ubiquitinated TDP-43 in frontotemporal lobar degeneration and amyotrophic lateral sclerosis. *Science.* 2006;314(5796):130–133.

3. Talbot K, Ansorge O. Recent advances in the genetics of amyotrophic lateral sclerosis and frontotemporal dementia: common pathways in neurodegenerative disease. *Hum Mol Genet.* 2006;15(supp 2):R182–R187.

4. Chen-Plotkin AS, Lee VM, Trojanowski JQ. TAR DNA–binding protein 43 in neurodegenerative disease. *Nat Rev Neurol.* 2010;6(4):211–220.

5. Geser F, Lee VM-Y, Trojanowski JQ. Amyotrophic lateral sclerosis and frontotemporal lobar degeneration: A spectrum of TDP-43 proteinopathies. *Neuropathology.* 2010;30(2):103–112.

6. Pesiridis GS, Lee VM-Y, Trojanowski JQ. Mutations in TDP-43.link glycine-rich domain functions to amyotrophic lateral sclerosis. *Hum Mol Genet.* 2009; 18(R2):R156–R162.

7. Buratti E, Baralle FE. Characterization and functional implications of the RNA binding properties of nuclear factor TDP-43, a novel splicing regulator of CFTR exon 9. *J Biol Chem.* 2001;276(39):36337–36343.

8. Ou SH, Wu F, Harrich D, Garcia-Martinez LF, Gaynor RB. Cloning and characterization of a novel cellular protein, TDP-43, that binds to human immunodeficiency virus type 1 TAR DNA sequence motifs. *J Virol.* 1995;69(6):3584–3596.

9. Arai T, et al. TDP-43 is a component of ubiquitin-positive tau-negative inclusions in frontotemporal lobar degeneration and amyotrophic lateral sclerosis. *Biochem Biophys Res Commun.* 2006;351(3):602–611.

10. Cairns NJ, et al. TDP-43 in familial and sporadic frontotemporal lobar degeneration with ubiquitin inclusions. *Am J Pathol.* 2007;171(1):227–240.

11. Winton MJ, Igaz LM, Wong MM, Kwong LK, Trojanowski JQ, Lee VM-Y. Disturbance of nuclear and cytoplasmic TAR DNA-binding protein (TDP-43) induces disease-like redistribution, sequestration, and aggregate formation. *J Biol Chem.* 2008; 283(19):13302–13309.

12. Kraemer BC, et al. Loss of murine TDP-43 disrupts motor function and plays an essential role in embryogenesis. *Acta Neuropathol.* 2010;119(4):409–419.

13. Sephton CF, et al. TDP-43 is a developmentally regulated protein essential for early embryonic development. *J Biol Chem.* 2010;285(9):6826–6834.

14. Wu LS, Cheng WC, Hou SC, Yan YT, Jiang ST, Shen CK. TDP-43, a neuro-pathosignature factor, is essential for early mouse embryogenesis. *Genesis.* 2010; 48(1):56–62.

15. Chiang PM, Ling J, Jeong YH, Price DL, Aja SM, Wong PC. Deletion of TDP-43 down-regulates Tbc1d1, a gene linked to obesity, and alters body fat metabolism. *Proc Natl Acad Sci U S A.* 2010; 107(37):16320–16324.

16. Tsai KJ, et al. Elevated expression of TDP-43 in the forebrain of mice is sufficient to cause neurological and pathological phenotypes mimicking FTLD-U. *J Exp Med.* 2010;207(8):1661–1673.

17. Wegorzewska I, Bell S, Cairns NJ, Miller TM, Baloh RH. TDP-43 mutant transgenic mice develop features of ALS and frontotemporal lobar degeneration. *Proc Natl Acad Sci U S A.* 2009;106(44):18809–18814.

18. Wils H, et al. TDP-43 transgenic mice develop spastic paralysis and neuronal inclusions characteristic of ALS and frontotemporal lobar degeneration. *Proc Natl Acad Sci U S A.* 2010;107(8):3858–3863.

19. Stallings NR, Puttaparthi K, Luther CM, Burns DK, Elliott JL. Progressive motor weakness in transgenic mice expressing human TDP-43. *Neurobiol Dis.* 2010;40(2):404–414.

20. Xu YF, et al. Wild-type human TDP-43 expression causes TDP-43 phosphorylation, mitochondrial aggregation, motor deficits, and early mortality in transgenic mice. *J Neurosci.* 2010;30(32):10851–10859.

21. Lim Y, Kehm VM, Li C, Trojanowski JQ, Lee VM-Y. Forebrain overexpression of alpha-synuclein leads to early postnatal hippocampal neuron loss and synaptic disruption. *Exp Neurol.* 2009;221(1):86–97.

22. Mayford M, Bach ME, Huang YY, Wang L, Hawkins RD, Kandel ER. Control of memory formation through regulated expression of a CaMKII transgene. *Science.* 1996;274(5293):1678–1683.

23. Gossen M, Bujard H. Tight control of gene expression in mammalian cells by tetracycline-responsive promoters. *Proc Natl Acad Sci U S A.* 1992; 89(12):5547–5551.

24. Hasegawa M, et al. Phosphorylated TDP-43 in frontotemporal lobar degeneration and amyotrophic lateral sclerosis. *Ann Neurol.* 2008;64(1):60–70.

25. Neumann M, et al. Phosphorylation of S409/410 of TDP-43 is a consistent feature in all sporadic and familial forms of TDP-43 proteinopathies. *Acta Neuropathol.* 2009;117(2):137–149.

26. Carter RJ, et al. Characterization of progressive motor deficits in mice transgenic for the human Huntington's disease mutation. *J Neurosci.* 1999; 19(8):3248–3257.

27. Komatsu M, et al. Loss of autophagy in the central nervous system causes neurodegeneration in mice. *Nature.* 2006;441(7095):880–884.

28. Miklyaeva EI, et al. Late onset Tay-Sachs disease in mice with targeted disruption of the Hexa gene: behavioral changes and pathology of the central nervous system. *Brain Res.* 2004;1001(1–2):37–50.

29. Ayala YM, Misteli T, Baralle FE. TDP-43 regulates retinoblastoma protein phosphorylation through the repression of cyclin-dependent kinase 6 expression. *Proc Natl Acad Sci U S A.* 2008;105(10):3785–3789.

30. Fiesel FC, et al. Knockdown of transactive response DNA-binding protein (TDP-43) downregulates histone deacetylase 6. *EMBO J.* 2010;29(1):209–221.

31. Strong MJ, et al. TDP43 is a human low molecular weight neurofilament (hNFL) mRNA-binding protein. *Mol Cell Neurosci.* 2007;35(2):320–327.

32. Iguchi Y, et al. TDP-43 Depletion induces neuronal cell damage through dysregulation of Rho family GTPases. *J Biol Chem.* 2009;284(33):22059–22066.

33. Li Y, et al. A Drosophila model for TDP-43 proteinopathy. *Proc Natl Acad Sci U S A.* 2010;107(7):3169–3174.

34. Jankowsky JL, et al. Persistent amyloidosis following suppression of Abeta production in a transgenic model of Alzheimer disease. *PLoS Med.* 2005; 2(12):e355.

35. Yoshiyama Y, et al. Synapse loss and microglial activation precede tangles in a P301S tauopathy mouse model. *Neuron.* 2007;53(3):337–351.

36. Balin BJ, Clark EA, Trojanowski JQ, Lee VM-Y. Neurofilament reassembly in vitro: biochemical, morphological and immuno-electron microscopic studies employing monoclonal antibodies to defined epitopes. *Brain Res.* 1991;556(2):181–195.

37. Igaz LM, et al. Enrichment of C-terminal fragments in TAR DNA-binding protein-43 cytoplasmic inclusions in brain but not in spinal cord of frontotemporal lobar degeneration and amyotrophic lateral sclerosis. *Am J Pathol.* 2008;173(1):182–194.

38. Guillemin I, Becker M, Ociepka K, Friauf E, Nothwang HG. A subcellular prefractionation protocol for minute amounts of mammalian cell cultures and tissue. *Proteomics.* 2005;5(1):35–45.